DOE/PC/95212--T3

DATE : January 15, 1997

TITLE : NOVEL TECHNIQUES FOR SLURRY BUBBLE COLUMN HYDRODYNAMICS

PI : M. P. Dudukovic', L. S. Fan

Co-Investigators : Dr. Y. B. Yang, and S. Degaleesan, P. Gupta (Graduate Students) (Washington University)
Dr. P. Jiang, and D. J. Lee, J. Reese (Graduate Students) (Ohio State University)
Dr. Min Chang (Exxon Research and Engineering)

INSTITUTIONS : Washington University, Chemical Engineering Department
Campus Box 1198, St. Louis, MO 63130-4899
(314) 935-6021;
Ohio State University, Department of Chemical Engineering
140 West 19th Avenue, Columbus, OH 43210
(614) 292-7907;
Exxon Research and Engineering
PO Box 101, Florham Park, NJ 07932-0101
(201) 765-6109

GRANT NO : DE-FG22-95 PC 95212

PERIOD OF PERFORMANCE : July 1, 1996 - December 31, 1996

Novel Techniques for Slurry Bubble Column Hydrodynamics

Semi-Annual Report for DE FG 22 95 PC 95212
July 1 – December 31, 1996

RECEIVED
AUG 18 1997
OSTI

I. Review of Objectives

The overall objectives of this cooperative University (Washington University and Ohio State University) – Industry (Exxon Research and Engineering) research are to provide experimental tools for measurement of important fluid dynamic quantities (at high pressure and temperature) and to verify phenomenologically or fundamentally based hydrodynamic models for scale-up and operation of slurry bubble columns.

The specific goals of this grant were listed in the previous annual report (July 1, 1995 – June 30, 1996) and are restated as follows:

Task 1. Develop computerized mathematical procedure (based on the physics of radiation and Monte Carlo calculations) for calibrating the Computer Automated Radioactive Particle Tracking Technique (CARPT) that will eliminate the existing lengthy in-situ calibration and allow the technique to be used in the field on high pressure units. Specifically, plan the use of CARPT on a high pressure bubble column such as the one available at Exxon Research and Engineering (ER&E) pilot plant facility in Florham Park, NJ.

Task 2. Improve the accuracy of the CARPT technique and compare the velocities obtained by CARPT in certain regions of the column to those determined by the Heat Transfer Probe and Particle Image Velocimetry (PIV).

Task 3. Develop probes for assessing local velocities, holdups and heat transfer coefficients in commercial bubble column reactors.

Task 4. Collect velocity and voidage profile data in gas-liquid and gas-liquid-solid systems at different solids loadings and at close to atmospheric pressure.

Task 5. Use state-of-the-art hydrodynamic models and codes to predict velocity and holdup fields under conditions studied experimentally. Search for most suitable constitutive forms (e.g., lift, drag, turbulence closure models, etc.) to reach agreement between calculated and experimentally observed values. Try to assess the effect of elevated operating pressure on various constitutive forms.

Task 6. Collect data in a high pressure 6" diameter bubble column such as the one available at ER&E, and compare to model predictions. Also collect high pressure PIV data in slurry systems at Ohio State University. Refine the hydrodynamic models if needed.

II. Summary of Accomplishments

The activities conducted as a part of this research at Washington University, Ohio State University and Exxon Research and Engineering during the period between July 1 to December 31, 1996 can be summarized as follows:

Washington University

1. Programs based on the Monte Carlo simulation for calibration of the Computer Automated Radioactive Particle Tracking (CARPT) technique are close to being completed. The following work has been accomplished during the last six months:

    a. A Monte Carlo program, to calculate the detector photo-peak and total efficiencies for any particle location inside the column and any detector location outside the column, was developed and encoded. Gaussian quadrature points were used for the surface integrals, resulting in fast and accurate computation of the detector efficiencies.

    b. A calibration (optimization) program to optimize the detector gains, detector dead-times, and media density has been written. The objective function is the sum of weighed least-squares between the measured detector-counts (from a few particle locations during calibration) and those calculated theoretically by above-mentioned Monte Carlo simulations, for the same particle locations as during calibration. It has to be emphasized that the number of calibration points required should be minimal, but at least equal to the number of detectors. To get accurate optimized values of the detector gains, detector dead-times, and media density, twice the number of detectors should be a good number to pick for the number of experimental calibration points. So, if one is using say 20 detectors for the experiment, then 40 calibration points should suffice. The General Reduced Gradient (GRG) technique is utilized to optimize the objective function. Two approaches were implemented : exact evaluation, and approximation in calculating the photopeak efficiency. The exact evaluation is very CPU intensive, and the approximation approach reduces the CPU time by two orders of magnitude.

    Once the optimized values of the detector gains, detector dead-times and the media density are obtained, one uses these optimized values, along with the detector peak and total efficiencies calculated by the Monte Carlo program, to calculate the entire calibration map for all the points on a dense 3-D grid. It is to be noted that the peak and total efficiencies have to be computed repeatedly for all the points on the 3-D grid. For this study, square cubic grids are used for the computation of this "efficiency" database, instead of non-uniform radial and azimuthal grids.

c. The inverse-mapping program to find the optimal location of the tracer particle from the dynamic count data and the "calibrated" 3-D mapping obtained by Monte Carlo simulation, was developed and implemented for a uniform distribution of media density. The program is very efficient in finding the grid point which yields the smallest chi-square value. After the grid point, which yields the smallest chi-square value, is found, 26 grid points in 3-D close to this grid point are located and their chi-square values are calculated. A 3-D interpolation scheme is then executed on the chi-square values of these 27 grid points. An optimization program (based on Powell's method) is used to find the local minimum of the chi-square and the corresponding particle location from the interpolation function. The interpolation is based on a 3-D quadratic function, and Powell's method is efficient in finding the local minimum of a quadratic function. The inverse-mapping program works for both uniform distribution of media density as well as for a non-uniform gas hold-up distribution of the type given by equation (1).

$$\varepsilon_g(\zeta) = \tilde{\varepsilon}_g\left(\frac{m+2}{m}\right)\left(1 - c\zeta^m\right) \tag{1}$$

This functional form is commonly adopted for the radial void fraction distribution. Here, m is the power law exponent, c is a parameter that allows for the observed non zero void fraction close to the wall and ζ is the dimensionless radius. The cross sectional mean void fraction is given by the relation :

$$\bar{\varepsilon}_g = \tilde{\varepsilon}_g\left(\frac{m+2-2c}{m}\right) \tag{2}$$

However, a non-uniform hold-up distribution requires that the Monte Carlo program be modified to account for the effective media density between the particle-detector pairs. Actually, for every particle-detector pair, 900 effective media densities have to be evaluated for the surface integral if 30 Gaussian points in one direction are used for calculating the photo-peak efficiency. A general equation was derived to calculate the effective media density between any two points located inside the column. The calculation of the effective media density involves an integral from the particle location to the location at the column wall at which the photons, emitted by the radioactive particle, exit the column and hit the detector. If the exponent m is equal to 2, an analytical expression for the integral can be obtained. However, if m is not equal to 2, the integral has to be evaluated numerically (this will increase the CPU time dramatically, since too many effective media densities have to be computed).

c. The work on a back-propagation neural network model to calculate the position directly from the counts recorded by the detectors during a CARPT experiment (i.e. performing real-time point-by-point reconstruction) has been initiated. The training set of data for the proposed network will be provided by the CARPT database and the predictions of the Monte Carlo simulation.

2. A phenomenological model for churn-turbulent bubble column.

a. A two bubble class gas-liquid recirculation 1-D model has been developed to simulate gas tracer responses in bubble columns operated under churn-turbulent conditions. Such a modeling effort is motivated by the recent findings of deSwart (1996). He measured, in a 2-D column, the interaction matrix between various large bubble sizes by a photographic technique, and set up a physically-based gas-liquid mass transfer model. The results show that the mass transfer coefficient based on such a model is approximately five times greater than that which would be estimated based on a single large bubble size. Thus, a better understanding of the interaction among various bubble sizes could lead to a more accurate estimation of the mass transfer coefficients, and subsequently to a better criterion for scale-up and design. deSwart's measurements of the interaction matrix were purely experimental, and this provides considerable motivation for theoretical prediction of such interactions. Also, one could not resort to photography as an experimental technique for the case of a 3-D churn turbulent column, as it is not possible to track individual bubbles in such dynamically coalescing and re-dispersing systems for lack of depth-of-view of any such photographic technique.

In the developed two-bubble class model, the interaction between the two bubble classes is accounted for through a coalescence-redispersion model. This requires an a priori information on bubble size distribution, which is the input necessary to calculate the coalescence and break-up rates of bubbles of various sizes, and subsequently, to estimate the overall interaction between the two bubble classes. The coalescence-redispersion model is based on the development presented by Luo (1993).

Simulation results have been obtained for the step input of tracer gas, while accounting for the interaction between the bubble classes in terms of an exchange coefficient. The capability to either measure or predict the bubble size distribution would enable one to calculate these exchanges based on Luo's coalescence-redispersion model. Alongside, work is in progress to formulate and subsequently simulate the 2-D version of the model.

b. A model is being proposed to get the least biased estimate of the bubble size and velocity distributions. This least-biased estimate is based on the principle of *Maximization of Shannon's Entropy*. Such a formulation requires as input the overall properties of the gas phase like the local holdup, the mean axial velocity, the variance of the velocity about the mean, the turbulent kinetic energy and a mean bubble size. These quantities can be computed from the steady-state solution to the two-dimensional axisymmetric two-fluid model. Thus, this is an indirect (approximate) method, as opposed to a complete population balance model, to simulate the size distributions as well as the overall properties like the liquid and gas velocity profiles, gas holdup and mass & heat transfer.

3. Attempts were made to measure the bubble size distributions using a one-point optical probe from Delft University (Groen *et al*, 1996). The encouraging outcome of the experiments was that the probe did not suffer from mechanical damage even in a slurry system with gas superficial velocities as high as 20 cm/s in an 8" column. For gas velocities in excess of 7 cm/s, the probe starts losing a lot more information, particularly on the larger sized bubbles. Thus, to get a better hold on the size distributions, a four-point probe is being fabricated at Delft University, and should be available for testing by the end of summer 1997. Figure 1 shows the working principle of the one-point optical probe.

Probe Characteristic Length, L_C (μm)

Bubble Rise Velocity, $V_B = L_C * t_R$ (m/s)

Length of Bubble Chord Pierced by Probe Tip, $L_B = V_B * t_B$ (mm)

Local Gas Hold-up, $\varepsilon_g \equiv \dfrac{\textit{Time Spent in Bubbles}}{\textit{Total Measurement Time}}$

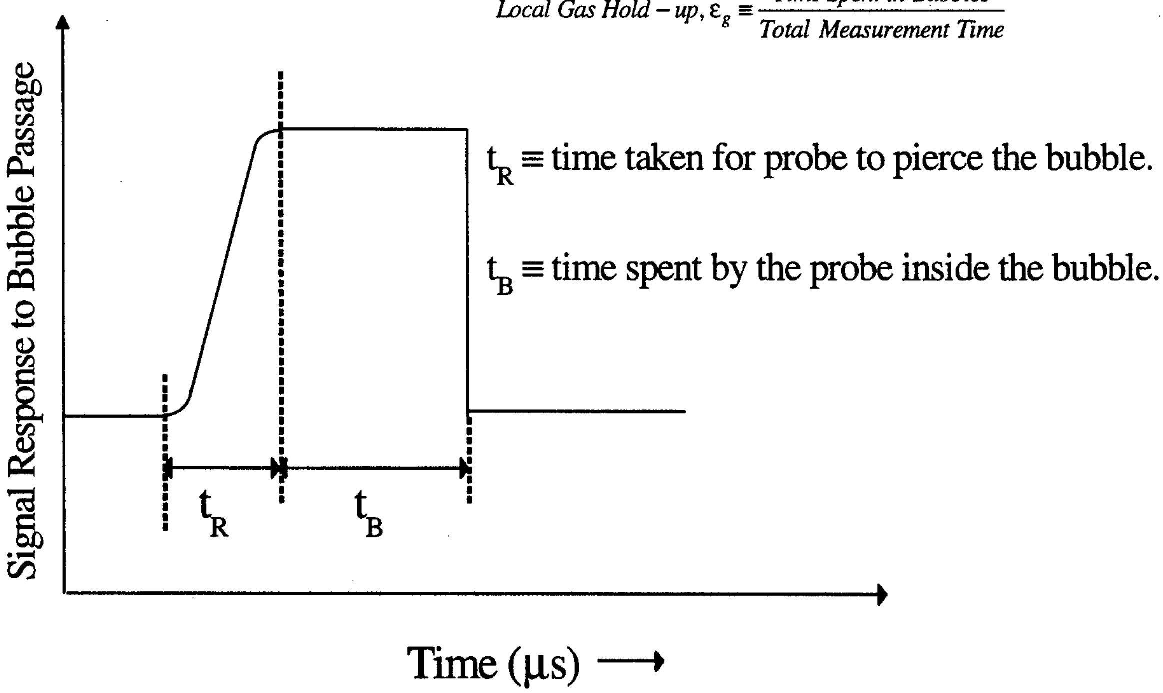

Figure 1 : Principle of One-Point Optical Fiber Probe.

4. A commercial Helium detector from Varian was tested for conducting gas tracer experiments in two as well as three-phase bubble columns operated under churn-turbulent conditions. Figure 2 shows the experimental set-up for the gas tracer experiment. Helium (the gas tracer) was injected below the distributor so as to achieve an almost uniform distribution of the tracer at the inlet, resulting from the high pressure drop across the distributor. The essential requirement of any equipment to be used for gas tracer experiments is that the response time of the detector should be at least around an order of magnitude less than the characteristic time of the system. Thus, the choice of the detectors for such experiments in churn-turbulent columns is very limited as the response time is the limiting factor.

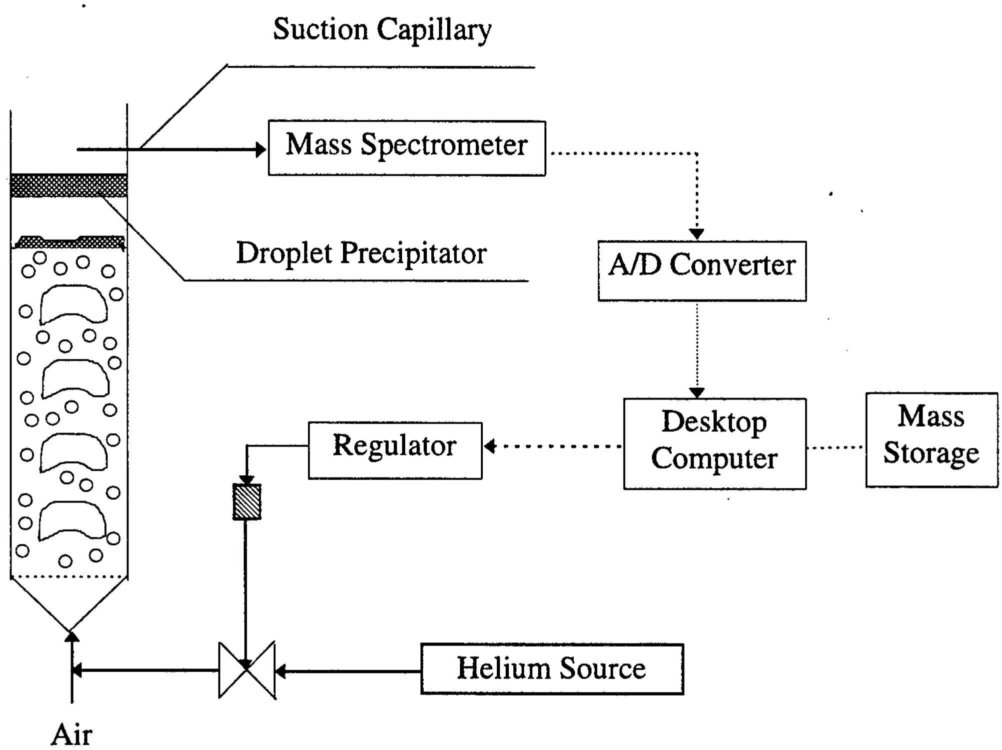

Figure 2 : Experimental setup for gas tracer experiment.

The response time of the detector tested was small enough to be able to give a satisfactory performance as indicated by the mean residence times for the two cases (Figure 3). Here, $\bar{t}_{calculated}$ is the mean residence time calculated based on the dynamic bed height and the superficial gas velocity, whereas $\bar{t}_{tracer\ curve}$ is calculated by an integral of [1-F(t)] over time.

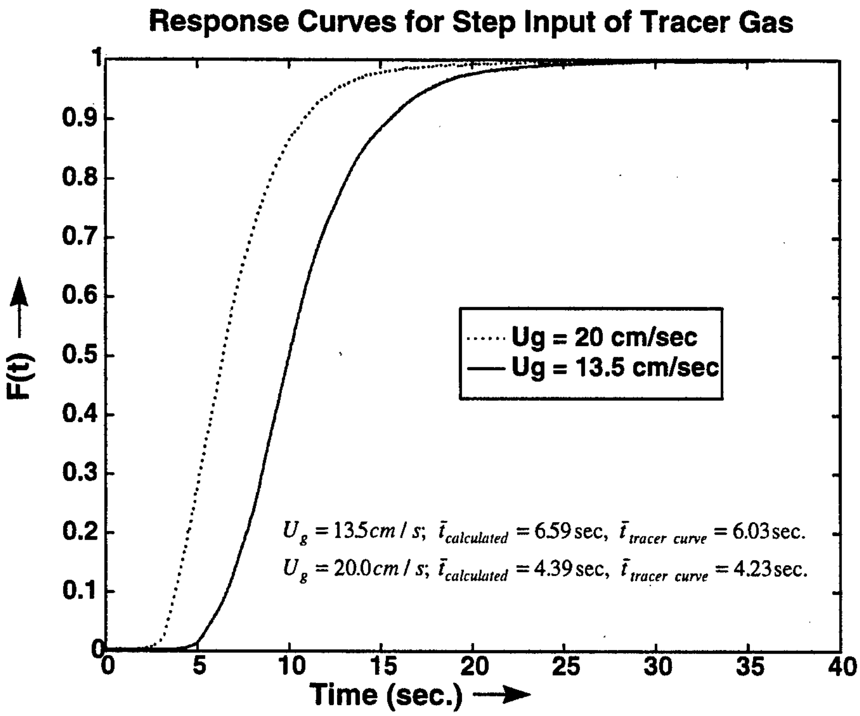

Figure 3 : Response curve of step input of gas tracer as measured by the Helium detector.

5. The calibration device for CARPT, described in the last annual report, for high pressure 6" column is under construction in the Medical School workshop at Washington University. As the gear belts, required as per the original design, were not available in the market, and the cost to custom machine it in the workshop was prohibitive, an alternative configuration for the same was proposed. Instead of using the gear belts, it was proposed to use a flexible stainless steel wire which is fixed along the length of the connected square rods. One end of the wire is connected to the bottom end of the calibration rod for support, while the other end is connected to the step motor. By winding the steel wire around a cylindrical drum, the step motor 2 drives the whole device up and down to get different axial positions. On the other hand, step motor 1 provides accurate azimuthal positioning of the calibration rod. A graduated scale is provided along the length of the calibration rod to ensure accurate axial positioning of the radioactive particle located at the tip of the calibration rod. Such a design is expected to have the same accuracy of positioning as the original one. A sketch of the new design is shown in Figure 4.

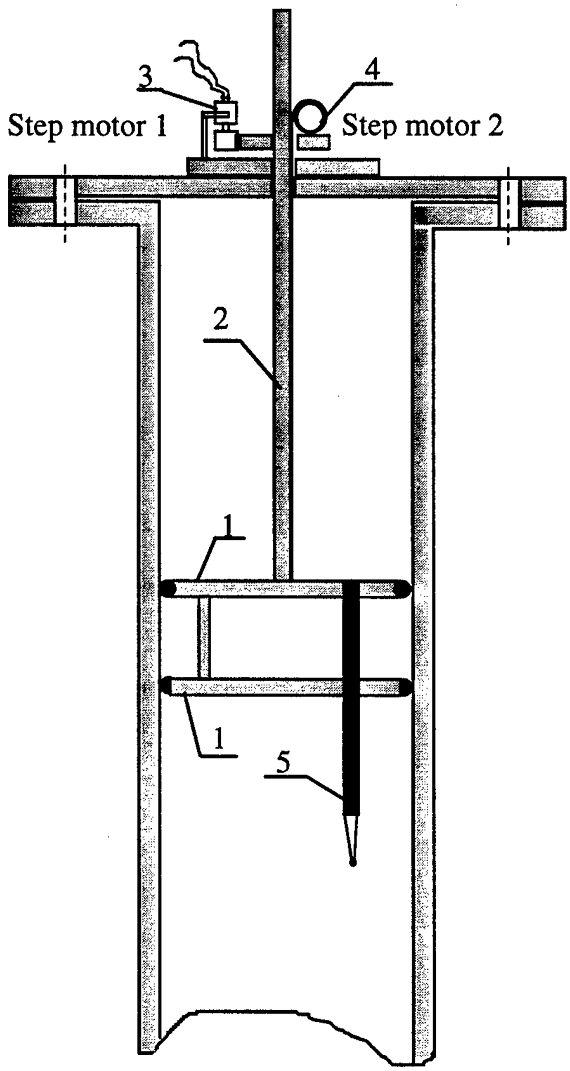

Figure 4 : Overall configuration of the modified calibration device.

Ohio State University

6. The Particle Image Velocimetry (PIV) technique, as developed by Chen and Fan (1992), is extended, combining the use of fluorescent seed particles and a proper isolation of illuminating lights, to obtain liquid flow fields more efficiently and more accurately. Particle images are created from light scattered by the seed particles. However, as might be expected, the scattered light is easily overwhelmed by scattering from other sources, such as interfaces between the bubbles and the liquid. This block-out of the light from the seed particles is most critical when the particles are located close to the bubbles. The use of fluorescent particles eliminates this problem by allowing spectral discrimination against scattered laser light. Fluorescence is a process in which light energy of one

wavelength is absorbed by a fluorescent material and then released as light energy of a slightly longer wavelength. When all the light entering the camera, with wavelengths lower than that of the emitted light from fluorescent particles, is filtered, the scattered laser light from the bubbles and background can be rejected.

A rectangular column made of plexiglas is used to demonstrate the effects of using fluorescent particles compared to non-fluorescent ones. The dimension of the column is 7.6 x 3.8 x 100 cm. Air is used as the gas phase and is distributed through a sparger. Distilled water is used as the liquid phase which is operated under batch conditions, and the static liquid height is kept constant at 80 cm from the bottom of the column for all runs. Neutrally buoyant Pliolite particles with a size range of 300 to 500 μm are used as the conventional liquid tracer. For fluorescent seed particles, dyed microspheres of polystyrene with 2% of divinylbenzene are selected. The mean diameter and the density of the microspheres are 250 μm and 1.062 g/cm^3, respectively. The dye is chosen to be well suited to the 515 nm bands of the argon laser. The flow field is illuminated by a laser sheeting technique. A 4W argon ion laser system is used as the laser source which is operated in a continuous mode, and a laser sheet of 3-5 mm thickness is created through the use of a cylindrical lens. The laser sheet is projected along the middle of the column to provide the distribution of liquid velocity. A high resolution (800 x 490 pixels) CCD camera equipped with variable electronic shutter ranging from 1/60 to 1/8000 of a second is used to record the image of the flow field. The fluorescent emission is isolated from the excitation light using a 5 cm round long pass filter mounted on the front of the camera. The cut-on wavelength of the filter is 530 nm. The image recorded by the CCD camera can be simultaneously digitized for immediate results on the flow field; moreover, can be connected to a S-VHS VCR for further study at a later time. An EPIX 4MEG VIDEO Model 12, 12 MIPS with 30 MHz max pixel clock and 17 MB on board memory is used to digitize the RS-170 analog voltage output from a CCD array or from a VCR.

The existing PIV technique and the modified PIV with fluorescent seeding particles and a proper isolation of lights are compared for various superficial gas velocities by obtaining profiles of the averaged velocity components and the Reynolds stress terms from many independent vector fields. Profiles are calculated by dividing the field of view into vertical strips that have a specified width and cover the entire height of the field of view. The familiar gross scale circulation is evident from the averaged velocity profiles, i.e. , a maximum upflow in the center and downflow closer to the wall. It is clearly shown that the profiles are the result of averaging the swinging (or swirling) motion of the central bubble stream and the related structures present, instantaneously, in the flow. From the same number of independent fields, although the velocity fields show similarity between two cases, except that the turn-around point is slightly pushed toward the wall when the non-fluorescent particle is used, the turbulence intensities generally decrease when the fluorescent technique is used. Especially, the decrease in the vertical normal stress is pronounced at the center of the column at which the fast bubble stream exists. The discrepancy between the two techniques increases with the gas velocity. When more independent fields are added to obtain the averaged velocity and the Reynolds stresses, the results from the two cases for lower gas velocities agree closely. However, for high gas hold-up, it is noted that many more independent fields are necessary to obtain the *final* profiles when the existing PIV data are compared with those from the modified one. The *final* profiles, thus obtained, become convincing when the results become insensitive to the number of analyzed independent vector fields. As mentioned earlier, the block-out, of the light from fluorescent tracers, due to the bubbles interferes with obtaining the 'true' liquid flow fields. In addition to the high velocities encountered in the bubble stream which make the matching of the triplets more difficult, the tracers are also frequently secluded or overwhelmed by a bubble or a cluster of bubbles. Note that the local gas holdup is much higher in the bubble stream in the center of the column than elsewhere. Without the filter to reject the light illuminated by the bubbles, the PIV suffers from the processes of discrimination and particle tracking in addition to the block-out of the tracers. In a thinner rectangular column, the discrimination between the phases is trivial since the object shows its actual size and shape, i.e. the interface is visible. However, when the laser sheet is projected along the 3-D column, the image of the illuminated object does not necessarily represent the actual shape of the object, particularly, when the shutter speed is high which is essential to track the fast moving liquid tracers. Thus, the PIV occasionally misidentifies the bubble as the seed particle. Moreover, as the gas rate increases, the systematic misidentification occurs more frequently because of breakup and coalescence of bubbles, formation of the cluster of bubbles, and small bubbles accumulated in the vortical structures. Consequently, the particle tracking cannot be performed efficiently and accurately to obtain the liquid flow field. As shown above, it is strongly asserted that the efficiency and the accuracy are dramatically increased by adopting the fluorescent technique for PIV. The modified PIV technique will be extended to measure liquid flow fields in a larger cylindrical column.

Exxon/Washington University

7. Based on the goals of this grant, Computer Automated Radioactive Particle Tracking (CARPT) and densitometry measurements were planned for the Exxon, 6'' diameter, high pressure, slurry bubble column at the ER&E pilot plant facility in Florham Park, NJ. Unfortunately, with preparations for this work in progress, it was discovered that Washington University's NRC license does not authorize the use of radioactive materials at any site other than those specified on its license which are within the main campus and the medical school facility of the university. Therefore, the radioactive materials such as Scandium-46 (activity level 200-450 μCi) and Cesium-137 (activity level 100 mCi) used by CREL under Washington University's NRC license for CARPT (Computer Automated Radioactive Particle Tracking) and CT

(Computer Tomography) respectively, cannot be moved for use at the Exxon high pressure slurry bubble column in Florham Park, NJ. The other alternative of Exxon obtaining a license for these radionuclides of the above mentioned activities, in order to implement CARPT/densitometry on the Exxon high pressure slurry column, did not work out either. ER&E's NRC license allows the possession and use of only the following radioisotopes : Carbon-14, Phosphorous-32, Phosphorous-33, Hydrogen-3 and Sulfur-35. None of these are suitable for the proposed work. Therefore, the Exxon radioisotopes committee recommended, based on NRC regulations, a third party to cover under its existing license for New Jersey the use of the needed isotopes at Exxon. Accordingly, CREL made extensive contacts with ICI Tracerco and Teledyne Brown Engineering. During the course of exploring these possibilities, it was realized that doing radioactive experiments at the Exxon pilot plant facility under a third party license would have the following disadvantages.

- Timing and scheduling : Third party license permits a limited level of radioactivity for a limited period of time. This would not allow CREL to perform a complete set of experiments designed to achieve the goals of this grant. In addition, the third party, Exxon and CREL had difficulties finding a mutually agreeable time period.
- Prohibitively high costs of involving the third party.

All of these made the planned investigations at Exxon unfeasible. Alternatively, ER&E and CREL have reached an agreement to build a high pressure, slurry bubble column at CREL, Washington University. The expenses of this endeavor are being borne by ER&E.

Setting up such a facility at CREL has many potential as well as immediately realizable advantages such as :

- CT scans of the entire high pressure column sections will be available which would not be the case had the experiments been performed at ER&E.
- As there are no timing and scheduling limitations, the complete set of experiments originally designed will be performed.
- Extensive CARPT/CT hardware does not need to be transported which will avoid any associated problems (e.g. change in hardware settings, damage, etc.).
- The facility will be permanently available for a wide range of future studies which would benefit all parties.
- The future access to the high pressure facility will not be proprietary.

All the required planning has been conducted and bids have been requested for installation of high pressure piping and building of a high pressure 6'' column at the Chemical Reaction Engineering Laboratory (CREL), Washington University.

References

Chen, R.C. and Fan, L.-S., 1992, "Particle image velocimetry for characterizing the flow structure in three-dimensional gas-liquid-solid fluidized beds", Chem. Eng. Sci., 47, 3615-3622.

Groen, J. S., Oldeman, R. G. C., Mudde, R. F. and Van Den Akker, H. E. A., 1996, "Coherent structures and axial dispersion in bubble column reactors", Chem. Eng. Sci., 51(10), 2511-2520.

Luo, H., 1993, "Coalescence, breakup and liquid circulation in bubble column reactors", Ph.D. Thesis, Universitetet I Trondheim, Norges Tekniske Hϕgskole

DeSwart, J.W.A., 1996, "Scale-up of a Fischer-Tropsch Slurry reactor", Ph.D. Thesis, University of Groningen, The Netherlands.

DISCLAIMER

M97054068

Report Number (14) DOE/PC/95212- -T3

Publ. Date (11) 19970115

Sponsor Code (18) DOE/FE, XF

UC Category (19) UC-101, DOE/ER

DOE